



This item was submitted to Loughborough's Institutional Repository by the author and is made available under the following Creative Commons Licence conditions.



CC creative commons
COMMONS DEED

Attribution-NonCommercial-NoDerivs 2.5

You are free:

- to copy, distribute, display, and perform the work

Under the following conditions:

BY: **Attribution.** You must attribute the work in the manner specified by the author or licensor.

Noncommercial. You may not use this work for commercial purposes.

No Derivative Works. You may not alter, transform, or build upon this work.

- For any reuse or distribution, you must make clear to others the license terms of this work.
- Any of these conditions can be waived if you get permission from the copyright holder.

Your fair use and other rights are in no way affected by the above.

This is a human-readable summary of the [Legal Code \(the full license\)](#).

[Disclaimer](#) 

For the full text of this licence, please go to:
<http://creativecommons.org/licenses/by-nc-nd/2.5/>

Probing bactericidal mechanisms induced by cold atmospheric plasmas with *Escherichia coli* mutants

Stefano Perni and Gilbert Shama

Department of Chemical Engineering, Loughborough University, Leics., LE11 3TU, UK

J L Hobman, P A Lund, C J Kershaw, G A Hidalgo-Arroyo and C W Penn

School of Biosciences, University of Birmingham, Edgbaston, Birmingham B15 2TT, UK

X T Deng, J L Walsh and M G Kong^{a)}

Department of Electronic and Electrical Eng, Loughborough University, Leics., LE11 3TU, UK

Mechanisms of plasma induced microbial inactivation have commonly been studied with physico-chemical techniques. In this letter, *Escherichia coli* K-12 and its $\Delta recA$, $\Delta rpoS$ and $\Delta soxS$ mutants are employed to discriminate effects of UV photons, OH radicals, and reactive oxygen species produced in atmospheric discharges. This microbiological approach exploits the fact that these *E. coli* mutants are defective in their resistance against various external stresses. By interplaying bacterial inactivation kinetics with optical emission spectroscopy, oxygen atoms are identified as a major contributor in plasma inactivation with minor contribution from UV photons, OH radicals, singlet oxygen metastables, and nitric oxide.

^{a)} Author to whom correspondence should be made, electronic mail: m.g.kong@lboro.ac.uk

Bio-decontamination using ionized gases has recently witnessed an exponential growth of interest, fuelled partly by an increasing challenge presented by bacterial and protein contamination¹⁻² and partly by the advent of atmospheric pressure glow discharges (APGD).³ Sustained in open air without the need of a vacuum chamber, APGD have been shown to inactivate many different microorganisms including the vegetative cells of yeast and bacteria, viruses, bacterial spores, and even biofilm-forming bacteria.⁴⁻⁷ A great deal has been learnt about how inactivation depends on the plasma operating conditions⁸ and the physiology of the microbial population.⁹⁻¹⁰ This has helped establish convincingly the microbiocidal capability of APGD. Much less understood are plasma inactivation mechanisms, an elucidation of which is central not only to the future development of the APGD bio-decontamination technology but also to the fledgling science of plasma-induced cellular manipulation.⁶ The current consensus is that chemically reactive species and UV photons generated in APGD are the most likely bactericidal agents with heat and electric fields playing only a minor role.¹¹⁻¹² The quest to uncover fully the identities of lethal plasma species has so far been inconclusive, though oxygen atoms have long been perceived as the likely main protagonists.¹² This owes partly to the difficulty in separating the production of different reactive APGD species and partly to the difficulty in measuring the absolute densities of these species. Alternative methodologies capable of contrasting out relevant plasma species and/or their effects are therefore highly desirable. In this letter, we employ wild type *Escherichia coli* K-12 and its mutants as bio-sensors for UV photons, OH radicals and reactive oxygen species to differentiate their individual roles with a view to ultimately unraveling APGD inactivation mechanisms.

E. coli K-12 MG1655¹³ single gene mutants were constructed using the method of Datsenko and Wanner,¹⁴ where a kanamycin resistance gene cassette was used to replace the *rpoS* gene, and a chloramphenicol resistance was used to replace the *recA* and *soxS* genes. Wild type *E. coli* K-12 strain MG1655 cells and $\Delta recA$, $\Delta rpoS$, $\Delta soxS$ mutants of this strain were stored and prepared as described elsewhere,¹⁰ except that the $\Delta recA$ and $\Delta soxS$ cells were

stored at 4°C on solid LB plates containing 100 µg/ml of chloramphenicol whilst the $\Delta rpoS$ cells were stored on plates containing 50 µg/ml kanamycin to select against loss of the antibiotic resistance genes that had replaced the *recA*, *soxS* or *rpoS* genes. For each strain, a loopful of cells was used to inoculate 100 ml fresh LB Broth with antibiotics as required, and at the concentrations given above, which were then incubated for 24 hours with shaking at 140 rpm. Cultivation under these conditions yielded final concentrations of approximately 10^9 colony forming units/ml. Cells were then deposited on 0.2 µm retention Whatman polycarbonate membrane filters of 25 mm diameter and dried in a laminar flow cabinet for 40 mins. The APGD system used here was essentially a plasma jet stuck inside a dielectric tube with a wrapped powered electrode and then ejected to a downstream grounded electrode,⁹⁻¹⁰ where the bacteria-laden membrane samples were placed. The gases used were helium (99.9999% purity) at a flow rate of 5 slm either alone or mixed with an O₂ flow at 5 sccm. Plasma excitation was through a 43.5 kHz sinusoidal source with a peak voltage of 4 kV, and the distance between the jet nozzle and the ground electrode was fixed at 3 mm. Plasma lethality was deliberately adjusted to be sub-maximal in order for differences in the responses of *E. coli* and its mutants to be detected. After plasma treatment, the membrane filters were placed in 10 ml of sterile Ringer's solution (Oxoid) and the cells detached by sonication for 15 seconds. Appropriate dilutions of treated bacterial suspensions were plated on LB Agar (supplemented with the recommended antibiotic in the case of *E. coli* mutants) and incubated for 24 hours at 37°C. All experiments were conducted in triplicate using three independent cultures.

Fig. 1 shows the results of APGD treatment when the working gas was helium only. In Fig. 1a, the inactivation kinetics of both the wild-type *E. coli* and its $\Delta recA$ mutant are seen to undergo approximately a 2.5 log reduction over 3 minutes of APGD treatment. The $\Delta recA$ mutants lack the *recA* gene which is associated with DNA repair.¹⁵ Given that UV photons exert their lethal effects by inducing DNA damage, the very similar susceptibility to APGD of the wild type cells and the $\Delta recA$ mutants suggests that little DNA damage was taking place, and

therefore there was an insignificant UV effect over the time course of the experiment. To understand the role of OH radicals, we employed the $\Delta rpoS$ mutant that lacks the *rpoS* gene and has a reduced resistance to OH radicals.^{17,16} APGD inactivation kinetics of the $\Delta rpoS$ mutants in Fig. 1b are very similar to that of the wild type, suggesting that OH radicals are unlikely to be important in the inactivation seen in Fig. 1a. As the *rpoS* gene also regulates aspects of *E. coli* resistance to environmental stresses such as heat, acid and salt,¹⁷ this result indicates that any thermal effects in our inactivation experiments are likely to be negligible.

Also shown in Fig. 1b is the APGD inactivation kinetics of the $\Delta soxS$ mutant, which suffers an 8 log reduction after 3 minutes of plasma treatment. This reduction becomes significant after 1.5 minutes. These results represent a clear contrast to the susceptibility of the wild type and the two other mutants to plasmas. The $\Delta soxS$ mutant lacks the *soxS* gene that regulates and is therefore required for *E. coli* resistance against reactive oxygen species, particularly nitric oxide (NO) and superoxide-generating agents.¹⁸ The observation of a very significant susceptibility of the $\Delta soxS$ mutants to APGD suggests that NO and/or superoxide-generating agents play a dominant role in the observed *E. coli* inactivation. As the $\Delta soxS$ mutant is most vulnerable to APGD, we use its kinetics against an unionized He flow as the control in Fig. 1.

It is possible that the relatively weak effect of UV photons and OH radicals in Fig. 1 is a consequence of sub-threshold dosage arising from the imposed plasma conditions. Under different conditions, and indeed in different APGD experiments, the production of UV photons and OH radicals could conceivably be more significant. It is therefore important to examine the generic applicability of the results in Fig. 1. This was done in our study by adding O₂ gas into the background He flow to modify the production of relevant plasma species. Fig. 2 shows the inactivation kinetics of the wild type and all three mutants when the background gas comprised a 5 slm He flow mixed with a 5 sccm O₂ flow. With the oxygen admixture, both the wild type and all three mutants suffer greater reduction in viability than the helium-only case of Fig. 1. The wild type together with the $\Delta recA$ and $\Delta rpoS$ mutants have very similar inactivation

kinetics, each achieving a 2.5 log reduction after 2.5 minutes of plasma treatment. This can only be explained if the plasma inactivation is dominated by reactive oxygen species. Similar to Fig. 1 on the other hand, the $\Delta soxS$ mutants suffer the greatest inactivation with an 8 log reduction after 2.5 minutes, shorter than the time scale of 3 minutes in Fig. 1. The onset point for the oxidative stress to become dominant is now earlier at 1.0 minute.

Although the use of *E. coli* mutants has enabled us to narrow down the most lethal species to two - nitric oxide and superoxide-producing agents - they are incapable of further discrimination. To this end, we employed optical emission spectroscopy (OES) to capture signatures of all major excited plasma species in the 200 – 1000 nm range. Fig. 3 shows the optical emission spectra for the He APGD and He-O₂ APGD, which exhibit strong emission lines of He species as well as UV, OH radicals, oxygen species and nitrogen species. The presence of the oxygen and nitrogen species arises because the APGD was ejected into the ambient air where its energetic electrons and metastables ionized and excited air molecules.^{12,1819} Although this creates a chemically reactive environment, the resulting plasma chemistry is often too complex for OES alone to unravel inactivation mechanisms.

By contrasting optical emission spectra under different plasma conditions and relating them to *E. coli* mutant inactivation data, valuable insights can be gained. As the O₂ flow rate is increased from 0 to 5 sccm, the data in Fig. 3 suggests that UV emission at 297.6 nm increases by 18.4% and UV emission measured by integrating over the 200 – 300 nm range increases by 7.5%. Despite this clear increase in UV production, the wild type and the $\Delta recA$ mutant share very similar inactivation kinetics as illustrated in Figs. 1 and 2. Therefore, for our gas plasma and possibly other He-O₂ APGD as well, UV production is likely to be too low to induce significant *E. coli* inactivation over the time scale of the experiment. This is consistent with a previous study using a UV-passing glass.¹² For the same increase in the O₂ flow rate, the OH emission intensity at 309 nm, 614 nm, and 616 nm is found to decrease by 66.1%, 20.6% and 75.5%, respectively. Given the increased inactivation of the $\Delta rpoS$ mutant with O₂ admixture,

the large reduction in OH emission intensities indicates a negligible role for OH radicals. Higher O₂ flow rates tend to reduce the OH intensity further (data not shown), thus suggesting that OH production may be too low in He-O₂ APGD to inactivate *E. coli* K-12 significantly.

Optical emission of excited-state NO species occurs at five wavelengths: 226.6, 236.3, 246.9, 270.9, and 283.1 nm,²⁰ of which the wavelength-integrated optical intensity increases by 8.3% when the O₂ flow rate was increased to 5 sccm. Although this increase is in line with the increase in plasma susceptibility of the $\Delta soxS$ mutant (Figs. 1 and 2), it contradicts the similar susceptibilities of the wild type and the UV-vulnerable $\Delta rpoS$ mutant. The 8-log reduction of the $\Delta soxS$ mutant may not therefore be caused by excited-state NO. We note that the main superoxide-generating agents are O₂(¹Σ_g⁺) and O₂(¹Δ_g) metastables as well as atomic oxygen. With increasing O₂ flow rate, the O₂(¹Σ_g⁺) line intensity at 760 nm is found to decrease by 44.8% and so is unlikely to be important. With its emission located between 1.2 and 1.3 μm, the O₂(¹Δ_g) metastable is much weaker than the O₂(¹Σ_g⁺) metastable²¹ and so is likely to be insignificant. For atomic oxygen on the other hand, its emission occurs at 615, 645, 725, 777 and 844 nm and by increasing O₂ flow rate, the line intensity at 777 and 844 nm increased by 38.0% and 29.3%, respectively with all three other lines reducing. As the $\Delta soxS$ mutant is more susceptible to superoxide-generating agents, the large increase of the line intensities at 777 and 844 nm offers a very strong case for a major role for oxygen atoms.

To compare more directly inactivation kinetics to OES, we employ the k_{max} parameter – the log reduction number per unit time at the beginning of plasma treatment.²² The wild type, the $\Delta recA$ and the $\Delta rpoS$ mutants are found in Fig.4a to have a similar k_{max} of about 1 log per minute, whereas the $\Delta soxS$ mutant has the largest k_{max} of 5.5 logs per minute. Compared to the 22% increase of k_{max} for the wild type, the negligible change in k_{max} of the $\Delta recA$ mutant suggests that UV photons and NO play only minor roles. The large increase of 55% for the $\Delta rpoS$ mutant does not correlate to the pervasive reduction in the OH line intensity in Fig. 4b. For the $\Delta soxS$ mutant, the increase of 24% in its k_{max} value correlates well with the 38.0%

increase at 777 nm and 29.3% at 844 nm in Fig. 4b. This suggests a dominant role for O atoms, particularly given that the strongest intensity of atomic oxygen lines is at 777 nm.

In conclusion, we have presented a plasma inactivation mechanism study using *E. coli* K-12 mutants as biosensors for key plasma species. By interplaying their inactivation kinetics with OES, we have identified the dominant role of excited oxygen atoms as well as minor roles for UV, OH radicals, O₂ metastables, and excited NO. Given the complexity of the APGD chemistry, additional studies are necessary, particularly on the role of ground-state O atoms, so as to enhance further the understanding of plasma inactivation mechanisms.

This research work is funded by Department for Environmental Food and Rural Affairs, UK and BBSRC grant EGA16107.

1. M. Laroussi, *IEEE Trans. Plasma Sci.* **24**, 1188 (1996).
2. X. T. Deng, J. J. Shi, H. L. Chen, and M. G. Kong, to appear in *Appl. Phys. Lett.*
3. U. Kogelschatz, *Plasma Chem. Plasma Processing*, **23**, 1 (2003).
4. H. W. Hermann, I. Henins, J. Park, and G. S. Selwyn, *Phys. Plasmas*, **6**, 2284 (1999).
5. N. S. Panikov, S. Paduraru,, R. Crowe, P. J. Ricatto, C. Christodoulatos, and K. Becker, *IEEE Trans. Plasma Sci.* **30**, 1424 (2002).
6. R. E. J. Sladek, E. Stoffels, R. Walraven, P. J. A. Tielbeek, R. A. Koolhoven, *IEEE Trans. Plasma Sci* **32**, 1540 (2004).
7. M. Vleugels, G. Shama, X. Deng, E. Greenacre, T. Brocklehurst and M. G. Kong, *IEEE Trans. Plasma Sci.* **33**, 824 (2005).
8. J. R. Roth, D. M. Sherman, R. B. Gadri, F. Karakaya, Z. Chen, T. C. Montie, K. Kelly-Wintenberg, and P. Y. Tsai, *IEEE Trans. Plasma Sci.* **28**, 56 (2000).
9. X. T. Deng, J. J. Shi, G. Shama, and M. G. Kong, *Appl. Phys. Lett.* **87**, 153901 (2005).
10. H. Yu, S. Perni, J. J. Shi, D. Z. Wang, M. G. Kong, and G. Shama, *J. Appl. Microbiology*, **101**, 1323 (2006).
11. M. Laroussi and F. Leipold, *Int. J. Mass Spectrometry*, **233**, 81 (2004).
12. X. T. Deng, J. J. Shi and M. G. Kong, *IEEE Trans. Plasma Sci.* **34**, 1310 (2006).
13. F. R. Blattner, G. Plunkett 3rd, C. A. Bloch, N. T. Perna, V. Burland, M. Riley, J. Collado-Vides, J. D. Glasner, C. K. Rode, G. F. Mayhew, J. Gregor, N. W. Davis, H. A. Kirkpatrick, M. A. Goeden, D.J. Rose, B. Mau and Y. Shao, *Science*, **277**, 1453 (1997).
14. K.A. Datsenko, and B.L. Wanner, *Proc. Natl. Acad. Sci. USA* **97**, 6640 (2000)
15. M. M. Cox, *Genes to Cells*, **3**, 65 (1998).
16. J. E. Visick and S. Clarke, *J. Bacteriology*, **179**, 4158 (1997).
17. A. M. Cheville, K. W. Arnold, C. Bushrieser, C. M. Cheng and C. W. Kaspar, *Appl. Environ. Microbiology*, **62**, 1822 (1996).
18. Z. Li and B. Demple, *J. Biological Chem.* **269**, 18371 (1994).
19. J. L. Walsh, J. J. Shi, and M. G. Kong, *Appl. Phys. Lett.* **88**, 171501 (2006).
20. A. Rahman, A. P. Yalin, V. Surla, O. Stan, K. Hoshimiya, Z. Yu, E. Littlefield and G. J. Collins, *Plasma Sources Sci. Technol.* **13**, 537 (2004).
21. J. Y. Jeong, J. Park, I. Henins, S. E. Babayan, V. J. Tu, G. S. Selwyn, G. Ding, and R. F. Hicks, *J. Phys. Chem.* **104**, 8027 (2000).
22. S. Perni, X. T. Deng, G. Shama, and M. G. Kong, *IEEE Trans. Plasma Sci.* **34**, 1297 (2006).

Figure captions:

FIG. 1: Inactivation kinetics by the helium APGD of wild type *E. coli* K-12 and its (a) $\Delta recA$ mutant; and (b) $\Delta rpoS$ and $\Delta soxS$ mutants. Control in (a) is the kinetics of the most vulnerable $\Delta soxS$ subject to a unionized He gas flow.

FIG. 2: Inactivation kinetics by the He-O₂ APGD of wild type *E. coli* K-12 and its (a) $\Delta recA$ mutant; and (b) $\Delta rpoS$ and $\Delta soxS$ mutants. Control in (a) is the kinetics of the most vulnerable $\Delta soxS$ subject to a unionized He-O₂ gas flow.

FIG. 3: Optical emission spectra of (a) the helium APGD and (b) the He-O₂ APGD at the sample point.

FIG. 4: As the O₂ flow rate increases from zero to 5 sccm, (a) k_{max} of wild type *E. coli* and mutants, and (b) percentage changes in optical emission intensities of different plasma agents with numbers indicating their emission wavelengths.

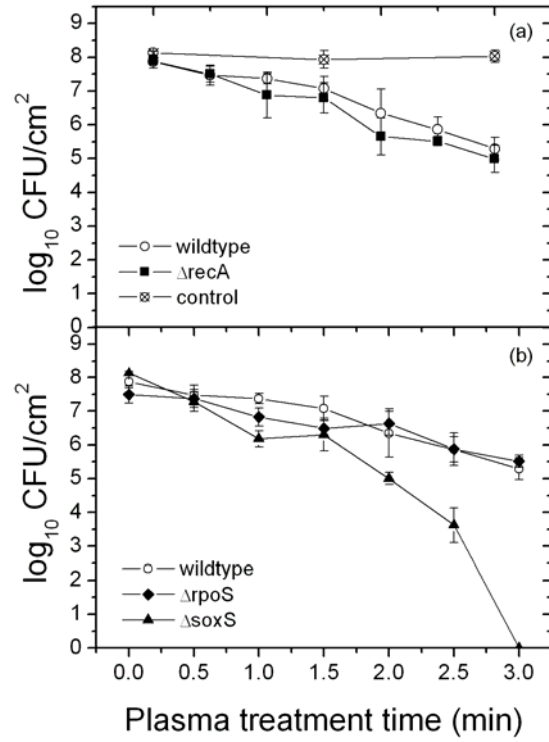


Figure 1: Inactivation kinetics by the helium APGD of wild type *E. coli* K-12 and its (a) $\Delta recA$ mutant; and (b) $\Delta rpoS$ and $\Delta soxS$ mutants. Control in (a) is the kinetics of the most vulnerable $\Delta soxS$ subject to a unionized He gas flow.

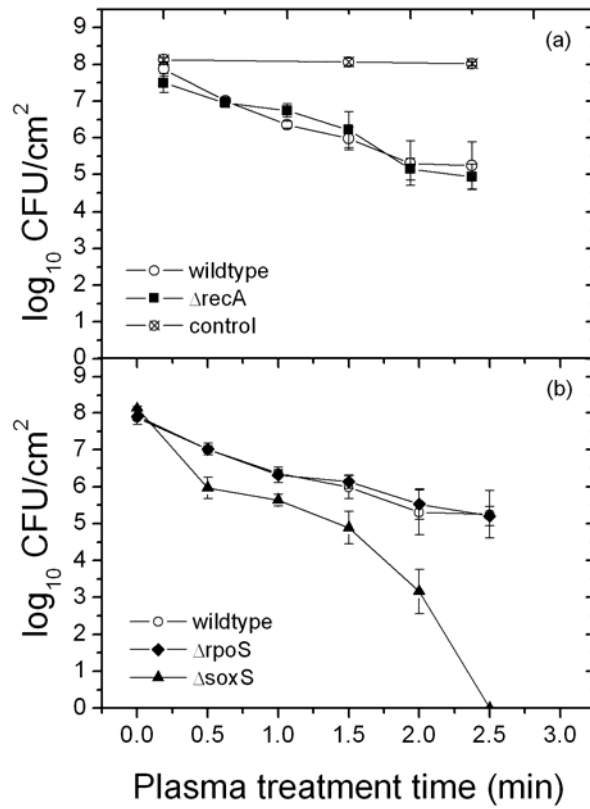


Figure 2: Inactivation kinetics by the He-O₂ APGD of wild type *E. coli* K-12 and its (a) $\Delta recA$ mutant; and (b) $\Delta rpoS$ and $\Delta soxS$ mutants. Control in (a) is the kinetics of the most vulnerable $\Delta soxS$ subject to a unionized He-O₂ gas flow.

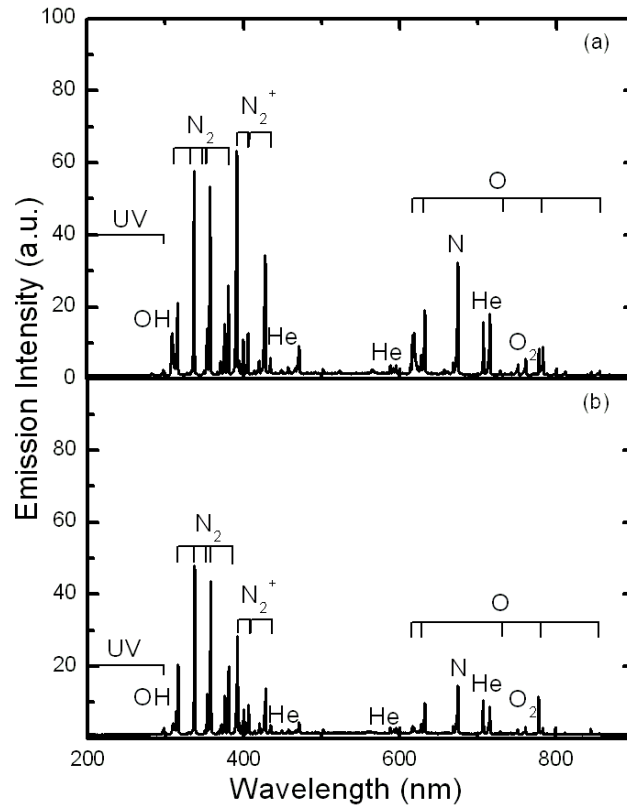


Figure 3: Optical emission spectra of (a) the helium APGD and (b) the He-O₂ APGD at the sample point.

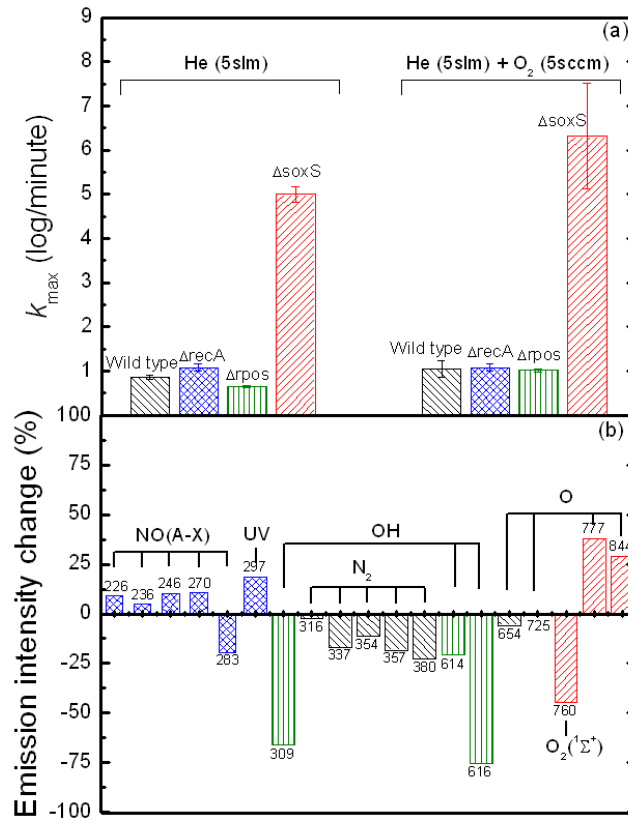


Figure 4: As the O₂ flow rate increases from zero to 5 sccm, (a) k_{max} of wild type *E. coli* K-12 and mutants, and (b) percentage changes in optical emission intensities of different plasma agents with numbers indicating their emission wavelengths.